

A deep focus on NGC 1883

A.L. Tadross*

National Research Institute of Astronomy and Geophysics, 11421-Helwan, Cairo, Egypt

Received 9 June 2005; accepted 9 August 2005

Abstract. A deep photometric analysis in the open star cluster NGC 1883 has been presented here and added to the work of Carraro et al. (2003), which is the only previous work introduced for this cluster. The radius and metallicity have been re-estimated in the present work. In addition, new parameters, namely luminosity function, mass function, total mass, mass segregation and the relaxation time of the cluster NGC 1883 have been estimated here for the first time.

Keywords : Galaxy: open clusters and associations – individual: NGC 1883 – astrometry – Stars: luminosity function – Mass function.

Open star clusters in the Galaxy are the key objects for studying the galactic structure and evolution, providing valuable information about star formation processes. The physical parameters of the clusters, e.g. distance, age, reddening and metallicity are required which can be derived from the colour-magnitude (*CM*) and colour-colour (*CC*) diagrams of the clusters. On the other hand the initial mass function (*IMF*) plays an important role in understanding the early dynamical evolution of star clusters, because it is a fossil record of the star formation process and provides an important link between the bright massive stars and the fainter low mass ones. Another related problem is the mass segregation in star clusters in which massive stars are more concentrated towards the cluster centre compared to low mass stars. It is not clear whether the mass segregation observed in several open clusters is due to dynamical evolution or an imprint of star formation processes itself or both (cf. Sagar et al. 1988; Sagar 2001 and references therein).

NGC 1883 (C 0522+465, OCL 417) is a northern open star cluster, located toward the anti-centre direction ($\alpha = 05^{\text{h}} 25^{\text{m}} 54^{\text{s}}$, $\delta = +46^{\circ}29'$, $l = 163^{\circ}.08$, $b = +06^{\circ}.16$, J2000). Trumpler (1930) suggested that this cluster is quite detached from the field, shows a clear

*e-mail: altadross@mailier.eun.eg

central concentration, and is moderately rich (I2m). Almost the same information can be obtained from Collinder (1931). Lyngå (1987) and Dias et al. (2002) report a preliminary estimate of NGC 1883 radius, amounting to 2.5-3.0 arcmin. The first time estimations of the fundamental parameters of NGC 1883, namely radial extent, age, distance and reddening, are performed by Carraro et al. (2003), hereafter CR03. They provided that the cluster has a radius of about 2.5 arcmin, as a lower limit, taking into account all the stars brighter than $V \approx 19.5$ mag.

On the basis of the fact that a cluster located towards the anti-centre might have a lower metal abundance than the Sun (Friel 1995), they used a theoretical isochrone of age = 1.0 Gyr and metal content $Z = 0.008$ (Girardi et al. 2000). The cluster fitting was quite good by shifting the isochrone with $E(B - V) = 0.35$, and $(m - M)_o = 13.40$ mag; ($R_V = 3.1$). NGC 1883 turned out to be located at 4.8 kpc from the Sun, 500 pc from the Galactic plane, and 13 kpc from the Galactic centre; ($R_\odot = 8.5$ kpc). The photometric data of CR03 is available in electronic form at the (WEBDA)¹ database, and the finding chart of NGC 1883 is taken from the Second generation Digitized Sky Survey (DSS-2)² archive.

1. About the present work

Depending on the *BVI CCD* photometry of CR03 and the Near-IR *JHK_s* data of the digital Two Micron All Sky Survey (2MASS)³, a deep stellar analysis in the open cluster NGC 1883 has been presented. 2MASS is uniformly scanning the entire sky in three near-IR bands *J*(1.25 μm), *H*(1.65 μm) and *K_s*(2.17 μm) with two highly - automated 1.3-m telescopes equipped with a three channel camera, each channel consisting of a 256×256 array of HgCdTe detectors. The photometric uncertainty of the data is < 0.155 mag with $K_s \sim 16.5$ mag photometric completeness. Further details are found at the 2MASS web site. Within a preliminary radius of 20 arcmin, stars extraction have been performed using VizieR⁴.

2. Completeness limits and field star contamination

To obtain comprehensive luminosity and mass functions, the data have to be corrected for completeness. In other words, the representative and non biased luminosity and mass functions can be constructed only if the data incompleteness is evaluated and removed. Fig. 1 shows that the completeness limit at 50%, which reached around $V = 18.8$ mag. At this level, the CR03 data can be cut-off (Sanner et al. 1999).

¹<http://obswww.unige.ch/webda/navigation.html>

²<http://cadewww.dao.nrc.ca/cadcbin/getdss>

³<http://www.ipac.caltech.edu/2MASS>

⁴<http://vizier.u-strasbg.fr/viz-bin/VizieR?-source=2MASS>

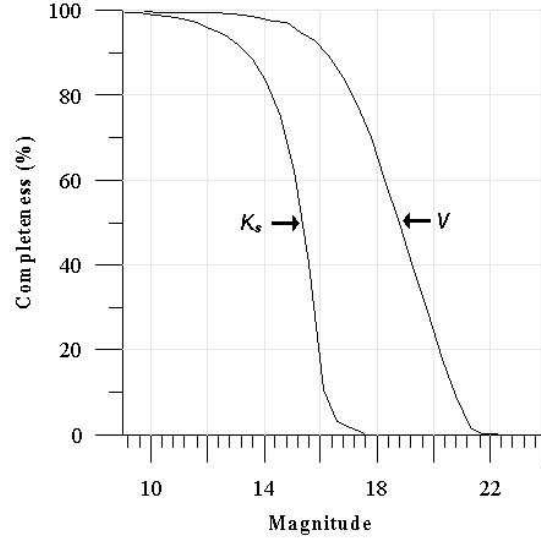


Figure 1. The completeness limit of NGC 1883 at level of 50% for V and K_s bands.

On the 2MASS scale, the completeness limits are found to be 16.5, 15.8, and 15.2 for J -, H -, and K_s -bands respectively. They are estimated from the luminosity function of each, where we consider the sample is completed up to the maximum bin. On the other hand, field star contamination has been checked using an adjacent field area ($\sim 1^\circ$ away from the cluster centre). Frequency distributions have been performed for the stars in K_s band of the cluster and field regions respectively. It is noted that the degree of field star contamination is increasing with faintness.

3. K_s radial profile

For determining the radial surface density of stars $\rho(r)$ in NGC 1883, the cluster area has been divided into a number of concentric circles (zones). The number density of stars, ρ_i , in the i^{th} zone has been calculated as $\rho_i = N_i/A_i$, where N_i is the number of stars and A_i is the area of the i^{th} zone (see Tadross 2005). Fig. 2 presents the K_s radial density profile, where only the sources brighter than the completeness limit were included. NGC 1883 presents a regular distribution falling steeply, the stellar surface density distribution exhibits a centrally condensed cluster. The background density corresponds to the average number of stars included in the field sample is found to be 3.0 stars per arcmin². Applying King (1962) model which is given for an open cluster as:

$$\rho(r) = \frac{f_0}{1 + (r/r_c)^2}$$

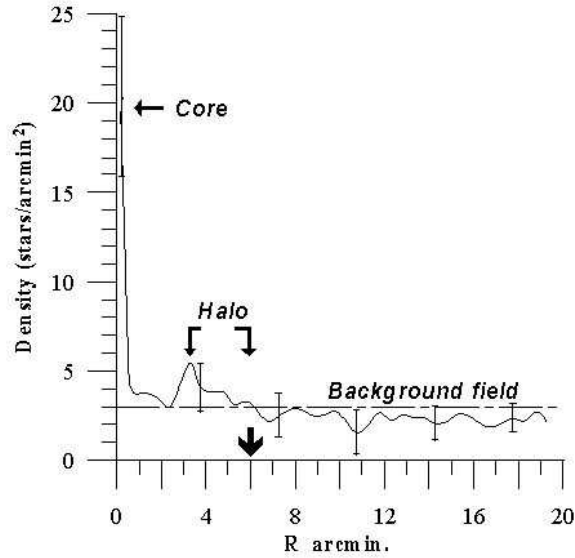


Figure 2. K_s -band radial profile of NGC 1883. The error bars represent the \sqrt{N} statistical error. The dashed line corresponds to the background field stars density. The core radius, the limited border, and the extended halo are marked with arrows.

where r_c is the cluster core radius and defined as the radial distance at which the value of $\rho(r)$ becomes half of the central density f_0 . The radial distribution of stars in NGC 1883 indicates that the extent of the cluster is 6.0 arcmin, and the value of the core radius derived in this way is found to be ~ 20 arcsec. The cluster size is thus many times larger than the corresponding core size which is in agreement with the findings of Nilakshi et al. (2002).

4. JHK_S CM-diagram and membership

The CM diagrams for various clusters given in the literature show that the density of faint members is usually comparable or even less than the field (background or/and foreground) population (Barrado y Navascués et al. 2001). On this respect, it is difficult to separate the field stars from the cluster members, only on the basis of their closeness to the main sequence of the CM and CC diagrams (Romeo et al. 1989). To know the actual number of cluster members from the remaining stars, precise proper motion and/or radial velocity measurements of these stars are required. In the absence of such data for faint stars, it is difficult to establish firmly their membership in the cluster. In this sense, according CR03 data, the photometric criterion for separating obvious field stars is applied. A star is considered as a non-member if it lies outside either the cluster radius or the cluster

main sequence *CM* diagram. The studied area of NGC 1883 is found to have 380 ± 10 stars.

On the 2MASS scale, the field stars contamination have been reduced after applying the completeness limit ($K_s < 15.2$ mag) to the stars inside the limited border of the cluster ($R < 6.0$ arcmin). According to Bonatto et al. (2005), the consequence of applying color-filter to the $K_s \sim (J - K_s)$ *CMD* has been performed whereas the stars located away from the *MS* have been subtracted. However, the resulting probable members are found to be 365 ± 20 stars (see Fig. 3), which are used to determine the physical parameters of NGC 1883.

5. Metallicity

J and K_s photometry allows us to obtain an independent estimate of cluster metallicity by means of the relationship between the spectroscopic metallicity and the Red Giant Branch (*RGB*) slope calibrated by Tiede et al. (1997). This relation correlates the abundance $[\text{Fe}/\text{H}]$ with the slope of the *RGB*, which can be written in the form:

$$[\text{Fe}/\text{H}] = -23.84(\pm 6.83) \times (\text{RGB slope}) - 2.98(\pm 0.70)$$

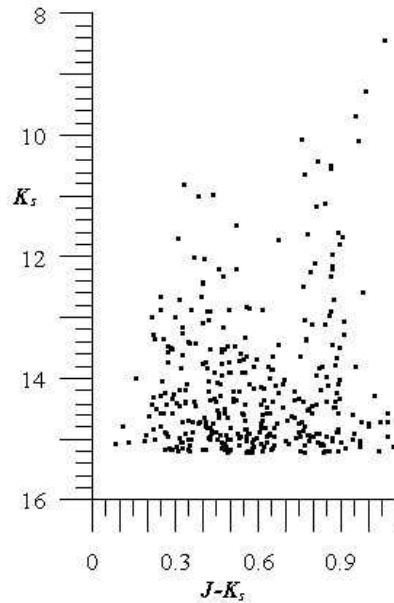


Figure 3. The color-magnitude diagram of NGC 1883 obtained using 2MASS data. The red giant branch (*RGB*) is appeared with prominent negative slope.

This relation has been proved to hold for both metal rich globular clusters and open clusters as well. For the latter, the RGB slope tends to present less negative values at decreasing age. We applied this relation to NGC 1883, for which the RGB slope is $\Delta(J - K_s)/\Delta K_s = -0.08 \pm 0.02$. This yields $[\text{Fe}/\text{H}] \sim -1.07$, which corresponds to a metal content of $Z_{\text{min.}}^{\text{max.}} = \left\{ \begin{matrix} 3 \times 10^{-3} \\ 6 \times 10^{-4} \end{matrix} \right\}$, (Bertelli et al. 1994). Although the brightest stars lie in the inner part of the cluster (within 3 arcmin only from the cluster center), some uncertainties may be detected because of the fitting error of the slope.

6. Luminosity function

To derive the true LF of the cluster, the field star contamination, with the other stars which are excluded by applying the colour filter, have been removed. The apparent magnitudes were converted into absolute magnitudes using the distance modulus of the cluster. A plot has been constructed for the cluster stars showing the number of stars at 0.5 intervals between observed magnitudes of 8 \sim 22 mag, as shown in Fig. 4. This size interval was selected so as to include a reasonable number of stars in each bin and for the best possible statistics of the luminosity and mass functions. The scale of the absolute magnitude appears on the upper axis of that figure. The visual total luminosity of the cluster is found to be -4.5 mag, where the high peaks lie at 5.4 and 1.8 mag for V and K_s bands respectively.

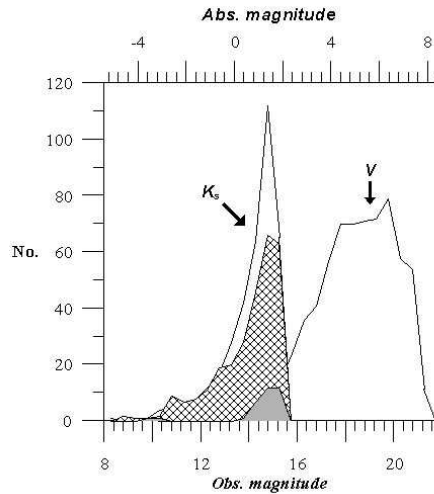


Figure 4. The luminosity function of NGC 1883 for V and K_s bands. Dashed and dark areas represent the field and colour-filter stars respectively. The absolute magnitude scale appears along the upper axis.

7. Mass function and total mass of NGC 1883

Given the luminosity function, the mass function and then the total mass of the cluster can be derived. To derive the *MF* from *LF*, we need theoretical evolutionary tracks and accurate knowledge of the cluster parameter, e.g. reddening, distance, age etc. Theoretical models of Girardi et al. (2000) and Bonatto et al. (2004) were used to convert the observed *LF* to the *MF* for *V* and *K_s* bands respectively. Step-plots have been constructed for the cluster stellar masses showing the number of stars at intervals between $0.9 \sim 1.8 M_{\odot}$, and $1.5 \sim 2.2 M_{\odot}$ for *V* and *K_s* bands respectively, as shown in Fig. 5. In these ranges, only stars brighter than the completeness limits and located inside the cluster radius, after excluding the field star contamination and applying the colour filter, the total mass of NGC 1883 is found to be $480 M_{\odot}$ and $650 M_{\odot}$ respectively. Using a least-squares fit, the slopes of *IMF* can be found as $\Gamma = -2.70 \pm 0.10$ and $\Gamma = -2.58 \pm 0.15$ for *V* and *K_s* bands respectively. From the luminosity function of the present day field stars, Salpeter (1955) derived the *IMF* with a slope of $\Gamma = -2.35$, assuming a constant rate of star formation and correcting for the stellar evolution, Tej et al. (2002). So we found that the present slopes of the *IMF* values are somewhat in agreement with the result of Salpeter.

It is noted that, on the other hand, unresolved binarity is a problem for this technique in two ways: A binary star that appears above the single star will be treated as one star

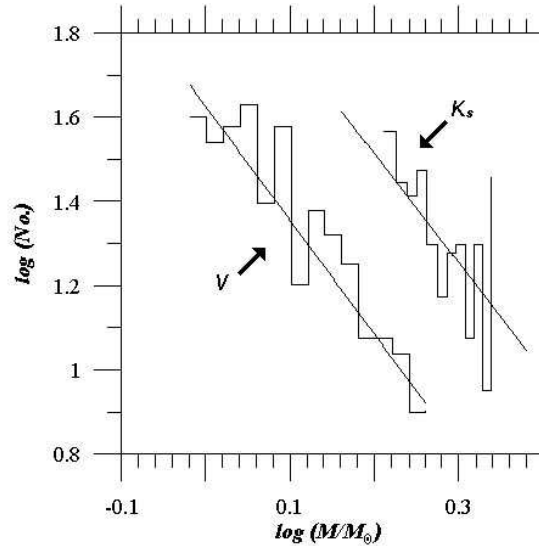


Figure 5. The mass function of NGC 1883 for *V* and *K_s* bands. The slopes of the *IMFs* are $\Gamma = -2.70 \pm 0.10$ and $\Gamma = -2.58 \pm 0.15$ respectively.

with a slightly higher mass than either of its two components. The second problem is that binary stars with unequal mass components will have a primary mass that is approximately correct, but the hidden, lower mass of the secondary component will not be included in the mass function, Naylor et al. (2002). In this respect, Van Albada & Blaauw (1967) estimated that 60% of early type stars are double systems, whereas Jaschek & Gomez (1970) claimed that approximately 50% of the *MS* stars are binaries (cf. Bernard & Sanders 1977). The average mass ratio of binary systems is given by Allen (1973) as $1.3 M_{\odot}$. In our case, according to the visual system (*V-band*), assuming the binary frequency is 50% of the *MS*, and taking the above value of Allen as the average stellar mass in NGC 1883, hence $\sim 200 M_{\odot}$ can be added to the cluster. This then gives a total cluster mass of $\sim 680 M_{\odot}$, which is very close to the value estimated from the second system (*2MASS K_s-band*).

8. Dynamical state and mass segregation

The evidence for mass segregation in a cluster may be seen from a plot of radius against the mass range of the cluster members. It is visible as a decrease of stars on the outer side of the cluster. For a dynamically relaxed cluster, the higher mass stars are expected to be settled toward the cluster centre, while the lower mass stars are residing in the outer regions of the cluster, Mathieu (1984). One would like to know whether existing mass segregation is due to dynamical evolution or imprint of star formation process. At the time of formation, the cluster may have a uniform spatial stellar mass distribution, which may be modified due to dynamical evolution of the cluster members. Because of dynamical relaxation, low mass stars in a cluster may possess largest random velocities, trying to occupy a large volume than the high mass stars do (Mathieu & Latham 1986, McNamara & Sekiguchi 1986, Mathieu 1985).

To display mass segregation in NGC 1883, star counts are performed on all members as a function of distance from the cluster centre and masses. The results are given in Fig. 6. The individual curves moving from left to right are for mass ranges $M/M_{\odot} > 2.0$, $1.5 \leq M/M_{\odot} \leq 2.0$, and $M/M_{\odot} < 1.5$. It suggests that the brighter high mass stars concentrate towards the cluster centre and accumulate much more quickly than the fainter low mass stars do.

The dynamical relaxation time, T_E which is the time in which the individual stars exchange energies and their velocity distribution approaches a maxwellian equilibrium can be estimated as

$$T_E = \frac{8.9 \times 10^5 N^{1/2} R_h^{3/2}}{\langle m \rangle^{1/2} \log(0.4N)}$$

where N is the number of cluster members, R_h is the radius containing half of the cluster mass and $\langle m \rangle$ is the average mass of the cluster stars (Spitzer & Hart 1971). The value of R_h has been assumed as half of the cluster radius derived here. Using distance, the angular value of the radius has been converted into linear value. In this way, the

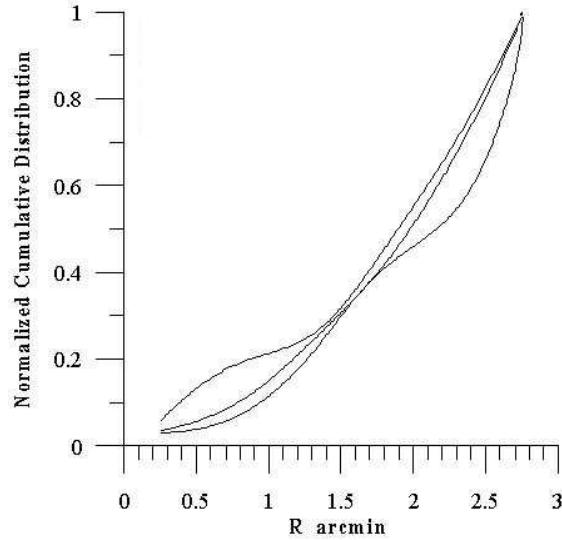


Figure 6. Mass segregation in NGC 1883. Moving from left to right, the curves represent the mass ranges $M/M_{\odot} > 2.0$, $1.5 \leq M/M_{\odot} \leq 2.0$, and $M/M_{\odot} < 1.5$. The bright massive stars accumulate much more quickly with radius than the faint low mass stars do.

dynamical relaxation time T_E has been estimated to be ~ 50 Myr, which implies that the cluster age is 20 times its relaxation one. However, the T_E value obtained here is considered as a lower limit value. Thus we can conclude that NGC 1883 is dynamically relaxed and the dynamical evolution is one of the possible causes of mass segregation.

9. Conclusions

Depending on the photometry of CR03 and $2MASS - JHK_s$ data, the present study leads to the following conclusions:

- (i) The radial density profile of NGC 1883 indicates that the extent of the cluster is 6.0 arcmin, and the value of the core radius is found to be ~ 20 arcsec.
- (ii) From the relation between the *RGB* slope and the metallicity calibrated by Tiede et al. (1997), it yields $[\text{Fe}/\text{H}] \approx -1.07$, which corresponds to a mean metal content of ~ 0.002 .
- (iii) The intrinsic luminosity function of NGC 1883 is constructed by subtracting field star contamination determined from neighbor field's. The visual total luminosity of the cluster is found to be -4.5 mag, where the high peaks lie at 5.4 and 1.8 mag for visual and $2MASS$ systems respectively.

- (iv) The mass function of NGC 1883 is constructed, and the slopes of *IMF* are found to be $\Gamma = -2.70 \pm 0.10$ and $\Gamma = -2.58 \pm 0.15$ according to visual and *2MASS* systems respectively. The total mass is found to lie between 480 and 650 M_{\odot} according to the visual and *2MASS* systems.
- (v) Mass segregation is observed in NGC 1883. The dynamical relaxation time T_E has been estimated to be 50 Myr, which indicates that NGC 1883 is dynamically relaxed and mass segregation may have occurred due to dynamical evolution.

Acknowledgements

It is worthy to mention that, this publication made use of WEBDA and the data products from the Two Micron All Sky Survey (2MASS), which is a joint project of the University of Massachusetts and the Infrared Processing and Analysis Center/California Institute of Technology, funded by the National Aeronautics and Space Administration and the National Science Foundation.

References

- Allen, C.W., 1973, *Astrophysical Quantities*, London, The Athlone Press.
- Barrado Y Navascués D., et al., 2001, *ApJSS*, **134**, 103.
- Bernard, J. Sanders, W.L., 1977, *A&A*, **54**, 569.
- Bertelli, G., et al., 1994, *A&AS*, **106**, 275.
- Bonatto, C., Bica, E., Girardi, L., 2004, *A&A*, **415**, 571.
- Bonatto, C., et al., 2005, *A&A*, **433**, 917.
- Carraro, G., Baume, G., Vilanova, S., 2003, *MNRAS*, **343**, 547.
- Collinder P., 1931, *Ld. An.*, **2**.
- Dias, W.S., Alessi, B.S., Moitinho, A., Lepine, J.R., 2002, *A&A*, **389**, 871.
- Friel, E.D., 1995, *ARA&A* **33**, 381.
- Girardi, L., Bressan, A., Bertelli, G., Chiosi, C., 2000, *A&AS*, **141**, 371.
- Jaschek, C. Gomez, A.E., 1970, *PASP*, **82**, 809.
- King, I., 1962, *AJ*, **67**, 471.
- Lyngå G., 1987, *The Open Star Clusters Catalogue*, **5th edition**.
- Mathieu, R.D., 1984, *ApJ*, **284**, 643.
- Mathieu, R. D., 1985, *Dynamics of star clusters*, **113**, 427 J. Goodman and P. Hut (eds.)
- Mathieu, R. D., Latham, D. W., 1986, *AJ*, **92**, 1364.
- McNamara, B. J. Sekiguchi, K., 1986, *ApJ*, **310**, 613.
- Naylor T., et al., 2002, *MNRAS*, **335**, 291.
- Nilakshi, Sagar, R., Pandey, A. K., Mohan, V., 2002, *A&A*, **383**, 153.
- Sagar, R., et al., 1988, *MNRAS*, **234**, 831.
- Sagar, R. 2001 in *IAU Symp.*, **207**, Extragalactic Star Clusters.
- Salpeter, E. E., 1955, *ApJ*, **121**, 161.
- Sanner, J., Geffert, M., Brunzendorf, J. Schmoll, J., 1999, *A&A*, **349**, 448.
- Spitzer, L. Hart M. H., 1971, *ApJ*, **164**, 399.
- Tadross, A. L., 2005, *AN*, **326**, 19.

- Tej, et al., 2002, *ApJ*, **578**, 523.
Tiede, G., Martini, P., Frogel, J., 1997, *AJ*, **114**, 694.
Trumpler, R.J., 1930, *Lick Observ. Bull.*, **14**, 154.
VandenBergh, D.A., 1985, *ApJS*, **58**, 711.
van Albada, T., Blaauw A., 1967, *CoORB, Uccle*, **B17**, 44.